AIAA-99-1469

CFD AND DOUBLET-LATTICE CALCULATION OF UNSTEADY CONTROL SURFACE AERODYNAMICS AND CORRELATION WITH WIND TUNNEL TEST

K. M. Roughen*, M. L. Baker†, and T. Fogarty‡
The Boeing Company, Long Beach, California 90807

Accurate prediction of control surface aerodynamics has been a challenge since the dawn of aviation. While this has been an important problem for many years, recent increases in the use of control surfaces for active control (load alleviation and flutter suppression) have increased the importance of accurate steady and unsteady control surface aerodynamics. Due to the strong influence of viscosity on the pressures on a trailing-edge control surface, the aerodynamic theories based on the linear potential equation have had only marginal success in predicting control surface aerodynamics, and in practice, large corrections (based on wind tunnel data) are often required for acceptable accuracy. Recent advances in computing technology and unsteady aerodynamic codes based on the Navier-Stokes equation are allowing more accurate analyses to be performed. In this paper, unsteady aerodynamic calculations due to control surface oscillations are made using a linear potential code (N5K) and a Navier-Stokes code (CFL3D.AE-BA). These computational results are compared to experimental unsteady pressure measurements, and the advantages of the nonlinear analysis are clearly demonstrated.

Introduction

With the increased interaction between the aerodynamic, structures, and controls disciplines in advanced aircraft, it is increasingly important to accurately predict the aerodynamic forces due to control surface deflection. The aerodynamic behavior of oscillating control surfaces has historically been difficult to predict analytically. The Doublet-Lattice Method (DLM)[1] has been the de-facto standard unsteady aerodynamic analysis tool in the subsonic regime for decades, but since it is based on the linear potential equation, it has had limited success in computing control surface aerodynamics. In practice, the aerodynamic results from the DLM (or a similar process) were modified using (sometimes large) correction factors[1] to improve correlation with test data. These correction factors are typically based on steady wind tunnel data, and are applied to steady and unsteady conditions alike. This is undesirable because the steady corrections will not necessarily be representative of the unsteady flow, and cannot correct the unsteady phase angle.

With the advent of low-cost, high-power computers, the use of unsteady Computational Fluid Dynamics (CFD) for the calculation of unsteady control surface aerodynamics has recently become more attractive. In this study, CFL3D.AE-BA[2] was used to compute unsteady Navier-Stokes solutions of oscillatory control surface motion. This model includes not only the effects of compressibility and transonic shocks, but also accounts for viscous effects.

Correlation of CFD to test data for the BACT model was accomplished by Schuster, et al.[3] with a ENS3DAE Navier-Stokes analysis. In the investigation discussed in this paper, the first step was to similarly validate CFL3D. The study performed by Schuster, et al. was used as another source of comparison for the validity of our CFD results.

For cases with small angle of attack and no deflected control surface, linear theory has been shown to be valid outside the transonic regime. When analysis is required for cases with an oscillating control surface, or for cases in the transonic regime, the validity of

---

* Intern, A&T Loads and Dynamics. Student, University of California at Los Angeles.
† Senior Engineer, A&T Loads and Dynamics. Member AIAA.
‡ Senior Engineer, A&T Loads and Dynamics.

linear theory breaks down. Flow characteristics are introduced which cannot be predicted by linear theory. A classic example of such flow characteristics occurs in the shock wave present for flows with a supersonic pocket at the surface of the wing. There will be a difference in the results obtained from linear theory and those obtained from test and CFD in the region upstream of the transition back to subsonic flow. Test data and CFD should predict an increase in phase lag in the unsteady pressure results. This behavior will be seen as near zero magnitude for cases in which the supersonic pocket has even higher velocity. This behavior will not be predicted by linear theory, and it is of the interest of this study to see at what Mach number and frequency of control surface oscillation this poor correlation begins to occur.

Wind Tunnel Model

In order to evaluate the accuracy of our analytical methods, it was necessary to compare them with test data. For this study, the Benchmark Active Controls Technology[4] (BACT) wing was used (fig. 1). The BACT model was tested in the Transonic Dynamics Tunnel (TDT) at NASA Langley Research Center. The model is a rectangular wing with NACA 0012 symmetric airfoil shape. The model has a trailing edge control surface extending from 45 percent span to 75 percent span. The control surface is located at 75 percent chord station. For testing purposes unrelated to our study, upper and lower surface spoilers were added with hingelines at the 60 percent chord station with the same spanwise dimensions and locations as the trailing edge control surface. Testing of the wing was conducted using R-12. For the steady state tests, the mean pressure measurements were available. For the unsteady tests the time history of the pressures were available and were converted to the frequency domain using a Fourier Transform on the last cycle. This yielded the pressure in terms of the response in phase with the flap motion (real) and 90 degrees out of phase from the flap motion (imaginary).

Pressures were measured at the 40 and 60 percent span locations. This study concentrates on the data collected at the 60 percent span location. There are 58 pressure orifices at this span location.

Analytical Models

For the analysis performed in this study, doublet-lattice and Navier-Stokes models were required. Since the BACT wing configuration is so simple, the DLM model consisted of a single panel broken down into 15 spanwise strips and 36 chordwise boxes. Based on the criteria in reference 1, this is expected to be valid up to a reduced frequency of kr = 2.0 for the M = .90 case.

For the Navier-Stokes solutions, a 3-D volume grid was required. The primary grid used in this study was a C-H topology with 557,685 grid points (153x81x45). This grid is shown in Figure 2. As will be observed, the resolution of this grid was not sufficient to capture all the details of the unsteady aerodynamics, but most of the correlation with the experimental results was admirable.

Process

Fourier Transform

The TDT data and the DLM results were originally available in terms of real and imaginary parts of pressure. The pressure data was converted to magnitude and phase using a spreadsheet. The results for the CFD runs were output in the time domain. In order to convert the output of CFL3D from time history to magnitude and phase, it was necessary to perform a Fast Fourier Transform on the results. This was done with a program developed by the Boeing Corporation. The output from this program gave the pressure results in terms of real and imaginary parts, which were converted to magnitude and phase in the same manner as for the TDT data and DLM results.

Pulse Input

For the results discussed in this study, the CFD runs were performed with an exponential pulse input. This was done to economize computer time. Fewer runs are needed for analysis using a pulse as compared to a sinusoidal input. This is due to the ability to convert to the frequency domain at multiple frequencies from a single run when using the pulse mode. The pulse runs, also require less time steps than do the sinusoidal runs, especially for low frequency cases. Sample time history pressure results are shown for both types of imput at one location on the wing for the Mach .77 case (fig. 3).

In order to examine the validity of the pulse input method, a case was analyzed using both pulse and sinusoidal deflection inputs for CFL3D. The results from this run are demonstrated in Figure 4. The run with pulsed input correlates acceptably well with the run with sinusoidal input. The magnitude results from the pulse run do not match the test data at the hingeline as well as do the results from the sinusoidal run. The phase results from the pulse run show noise toward the leading edge, this was not present in the results from the sinusoidal run. Due to the presence of noise near the leading edge of the run performed with pulse input, the CFD results at the leading edge

are not shown in plots elsewhere in this paper. In order to obtain acceptable results near the leading edge, sinusoidal runs would need to be performed for all cases.

Results

Steady State Results

The results obtained from the steady state runs of CFL3D were observed for all Mach numbers studied. These results have been included along with test data in Figures 6, 10 and 14. The steady results agree reasonably well with the test data for all cases being studied. The shock present in the M=.82 case is predicted to be larger and farther aft than is seen in the test data.

Unsteady Results with Pulsed Aileron

This study concentrated on zero angle of attack cases ranging from a frequency of 2 Hz to a reduced frequency of 1.0. The range in which the test data and both methods of analysis were studied is illustrated in Table 1. Several observations can be made from the results shown in Figures 5 through 17.

Mach 0.65

For the purely subsonic condition shown in Figures 5 through 8 (Mach 0.65), there is relatively good agreement between the doublet-lattice results, the Navier-Stokes results, and the test data. This is not surprising, as the flow is entirely subsonic and well behaved (fig. 5). The magnitude of the unsteady pressure as computed by the doublet-lattice method is fairly close to the experimental results, but there are areas where the doublet-lattice method clearly does not contain the relevant physics. The most obvious is the peak in unsteady pressures at the leading edge which is absent from the experimental data. The pressure distribution on the flap itself (aft of the hingeline) also shows significant deviation from the experimental results. One area of surprisingly good correlation between doublet-lattice and wind tunnel results is the unsteady pressure at and immediately forward of the hingeline itself. The prediction of the unsteady pressure phase angle from doublet-lattice is also fairly good, but deviates from the experimental results aft of the control surface hingeline.

The Navier-Stokes results, as expected, show somewhat better correlation with the test data. The leading edge peak in unsteady pressure that was seen in the doublet-lattice results is absent from the Navier-Stokes solutions. The pressure magnitude distribution on the flap itself is much closer to the experimental results than the doublet-lattice was, and the pressures on the airfoil forward of the hingeline are in excellent agreement with the experimental data. The correlation of the unsteady pressure peak at the hingeline itself is disappointing, however, with the Navier-Stokes results showing significantly lower peaks than the test data. This is due to a relatively coarse CFD mesh in the chordwise direction in the vicinity of the hingeline. The correlation of the unsteady phase angle is similar to the doublet-lattice results. There is good agreement with the experiment except on the flap itself. Since the magnitude of the unsteady pressures is so small in this region, this represents a relatively minor inaccuracy, and it is not certain that the experimental results are meaningful.

At higher reduced frequencies, the discrepancies between the unsteady pressure magnitudes seen in the doublet-lattice and Navier-Stokes results are seen to diminish until, at a reduced frequency of k=1.0, there is almost no difference except at the hingeline. This observation is consistent with the industry practice of rolling off “knockdown factors” as reduced frequency increases. However, the results show increasing discrepancies in the phase angle of the unsteady pressures with higher reduced frequencies.

Mach 0.77

Transonic effects begin to become apparent in these results. For the most part, the observations about the results and the qualitative correlation between doublet-lattice, Navier-Stokes, and experimental results are similar to the subsonic results. However, there are some important differences that appear in the neighborhood of the supersonic pocket. Figure 9 shows Mach contours of the steady-state solution in the plane of the pressure measurements. The region from approximately 10% to 40% chord has supersonic flow, but the downstream termination of the supersonic region is a gentle recompression, rather than a shock. However, the fact that the flow is locally supersonic causes a significant change in the upstream propagation of information. This is most clearly seen in the unsteady pressure phase plots in Figures 11 and 12. While in the subsonic case, the phase shows a fairly linear variation upstream of the hingeline (governed by upstream propagation of information), the supersonic results clearly show nonlinear behavior. There is an inflection point in the phase-vs.-chord plots at approximately 30% chord. This roughly corresponds to the location where an upstream-traveling signal would encounter supersonic flow. The signal must, in effect, travel around the supersonic region to influence surface pressures, which causes an increased phase lag. This results in a steeper slope in the phase-vs-chord curve in the supersonic region. This gradually levels out near the leading edge, where the flow is again

subsonic. There is excellent qualitative agreement between the experimental and Navier-Stokes results in this area.

The effect of the supersonic pocket can also be seen in the magnitude plots of the Navier-Stokes results. There is clearly a "bump" in the unsteady pressure magnitude at approximately 20% chord, which corresponds to the recompression region.

Behavior aft of the hingeline is similar to that seen in the subsonic case, with the Navier-Stokes results showing better magnitude results than the doublet-lattice method.

The effects of increasing the amplitude of the unsteady flap motion can be seen in Figure 17. In these analyses, the flap motion had a maximum amplitude of 4 degrees.

Mach 0.82

The steady Mach contours in Figure 13 show the presence of a transonic shock at approximately 40% chord in the Mach 0.82 case. The presence of the shock is also clearly evident in the steady-state pressure distribution shown in Figure 14. The effects of the shock are also quite obvious in the unsteady pressure results. In the unsteady pressure magnitudes, there is a clear peak in the unsteady pressure at approximately 35% local chord in the experimental results, and at 40% local chord in the Navier-Stokes results. The peak, which represents the "shock doublet" caused by unsteady chordwise motion of the shock, is absent in the linear doublet-lattice results. Quantitatively, the correlation of the shock doublet peak between experimental and Navier-Stokes results is disappointing. The CFD results predict a shock doublet of approximately double the amplitude of that seen in the experimental results. This indicates that the shock in the CFD solution is somewhat stronger than that found in the experiment. This may be due to the choice of turbulence models used in the CFL3D analysis.

A similar phenomenon is seen in the phase angle of the unsteady pressures. There is a clear discontinuity in the phase angle across the shock in both the experiment and the Navier-Stokes analysis. However, the magnitude of the discontinuity in the Navier-Stokes solution is significantly larger than that seen in the experiment.

Correlation between the CFD solutions and the experiment is excellent away from the neighborhood of the shock. Forward of the shock, both the CFD and the experiment show almost no unsteady pressure fluctuations due to the large supersonic region,. Aft of the shock, the magnitude correlation is excellent, including the peak at the hinge line and the pressures on the flap itself. Consistent with the other Mach numbers, the phase of the experimental pressures on the flap does not agree with the analysis, but this is not very significant due to the extremely low pressure magnitudes in this region.

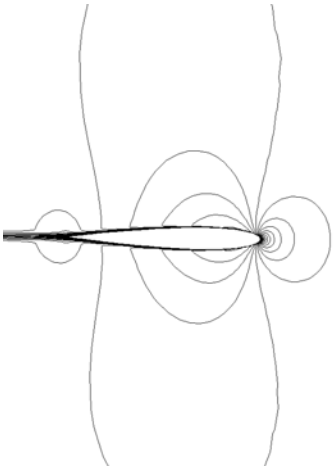

Figure 5- Mach contours for $M_\infty = .65$

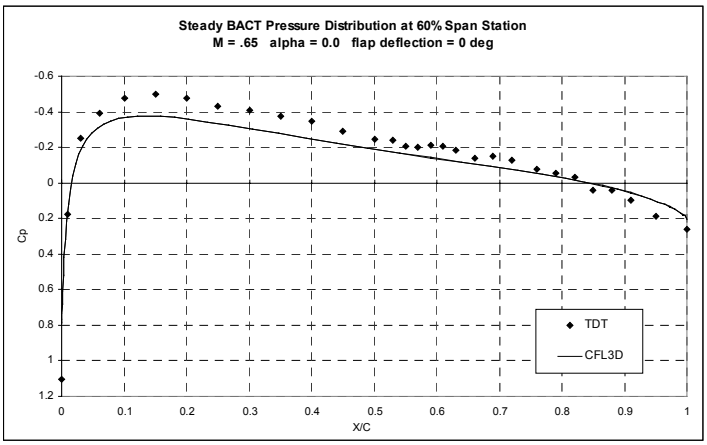

Figure 6- Steady Pressure Coefficient for $M_\infty = .65$

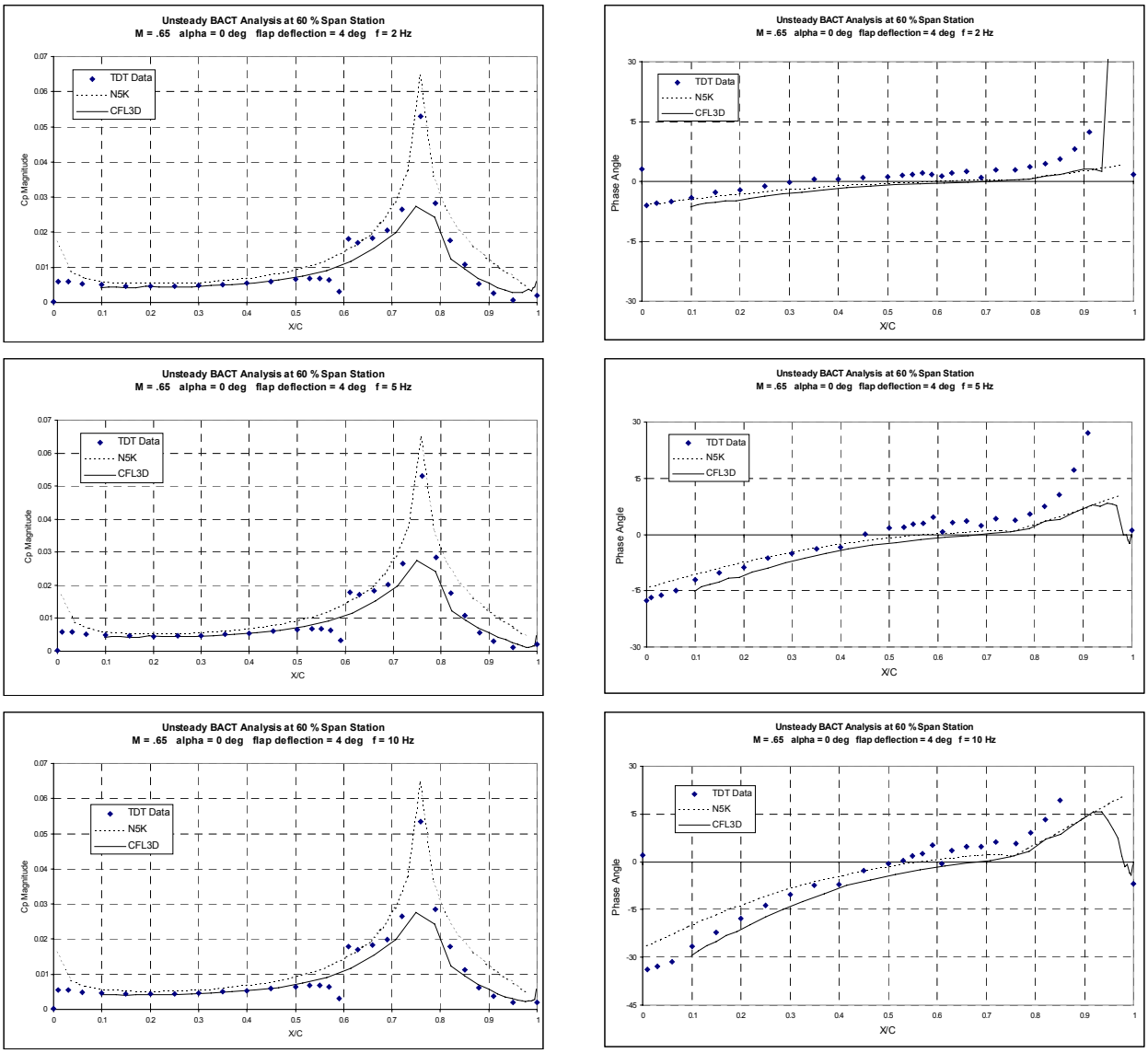

Figure 7- Unsteady Pressure Coefficient from 2 to 10 Hz

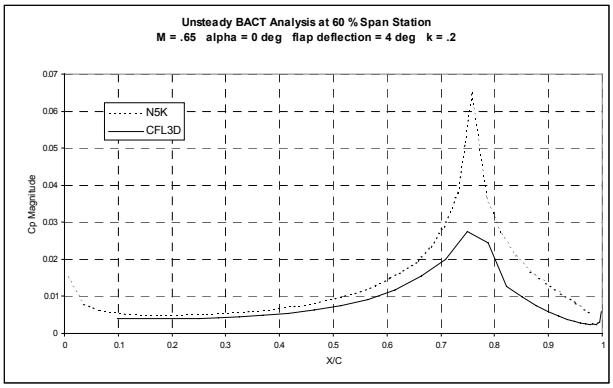

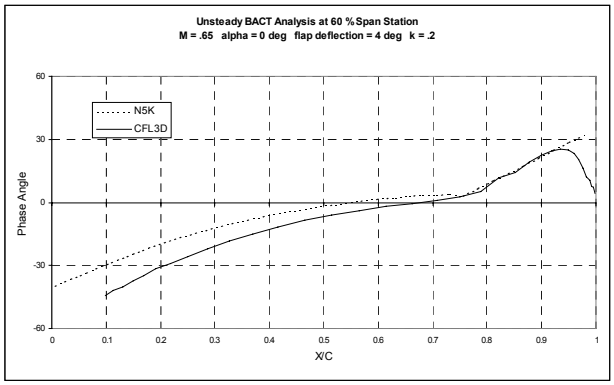

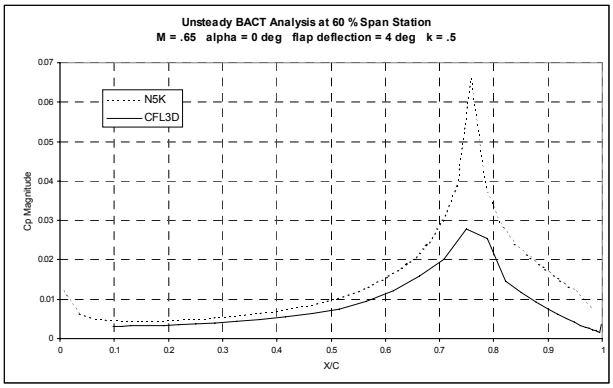

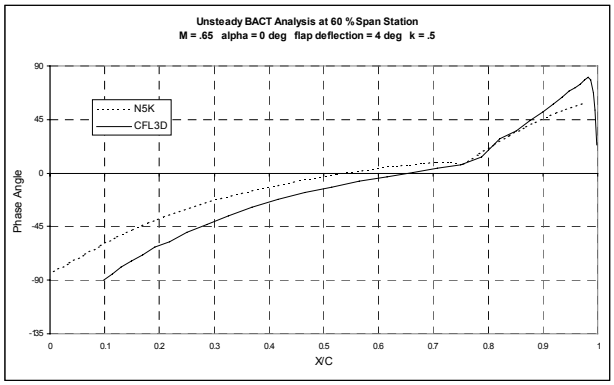

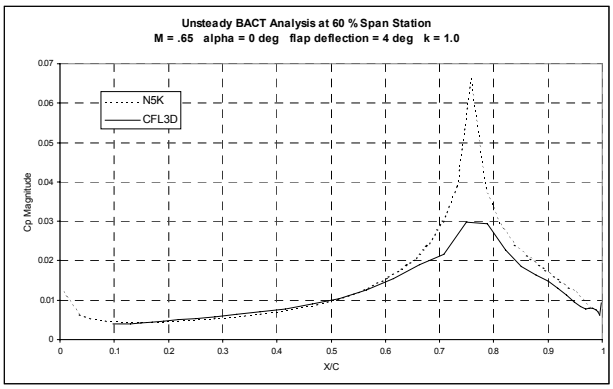

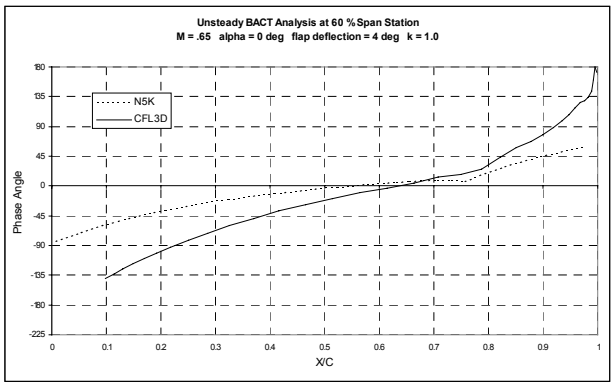

Figure 8- Unsteady Pressure Coefficient for reduced frequency from 0.2 to 1.0

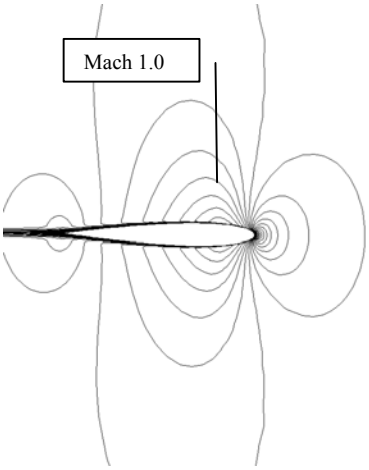

Figure 9- Mach contours for $M_\infty = .77$

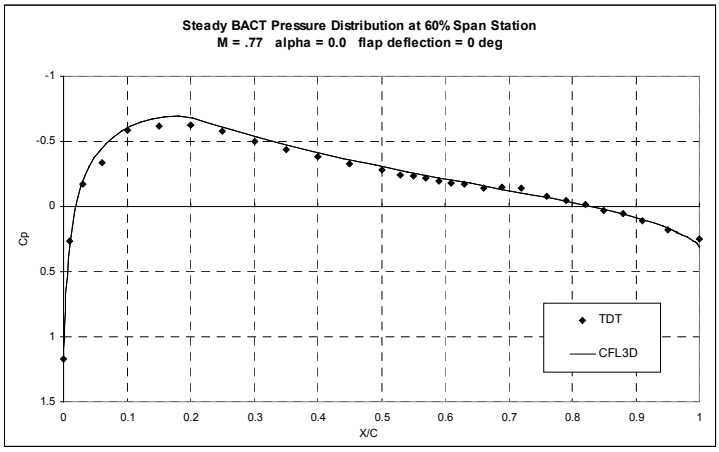

Figure 10- Steady Pressure Coefficient for $M_\infty = .77$

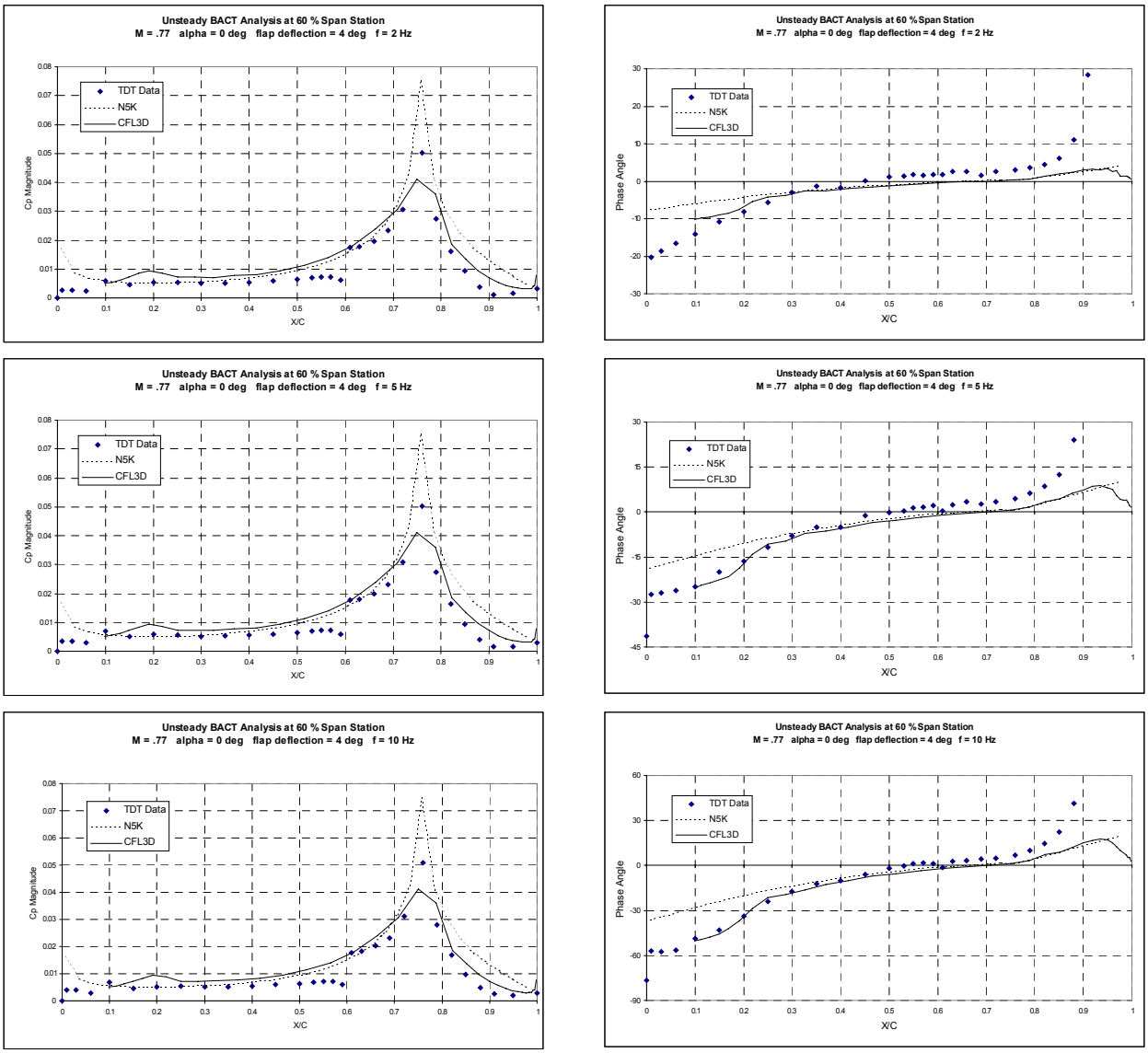

Figure 11- Unsteady Pressure Coefficient from 2 to 10 Hz

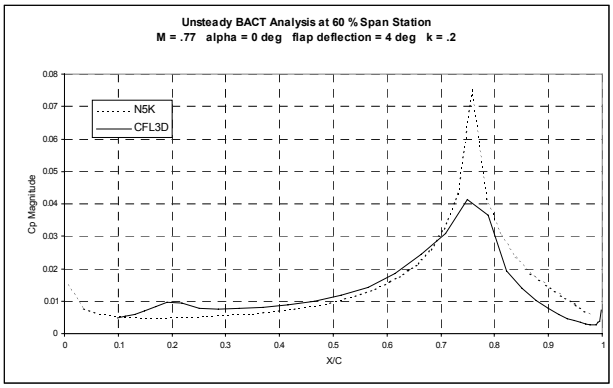

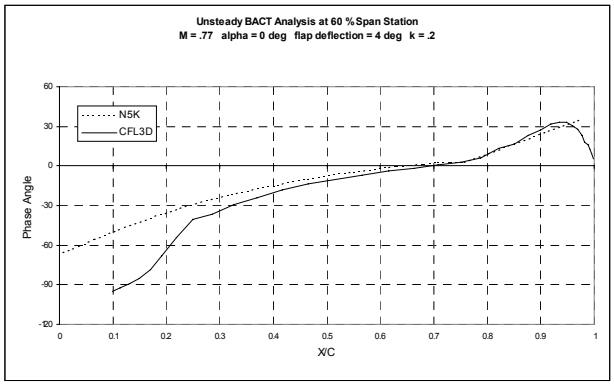

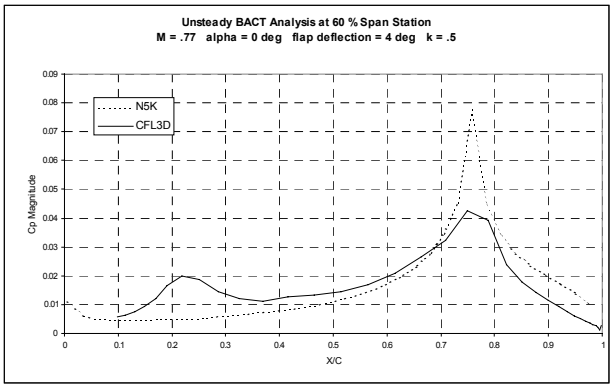

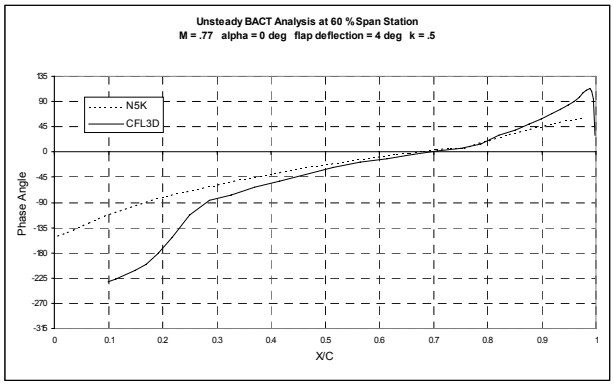

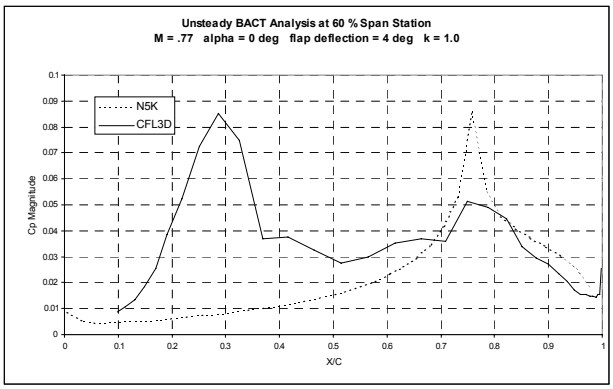

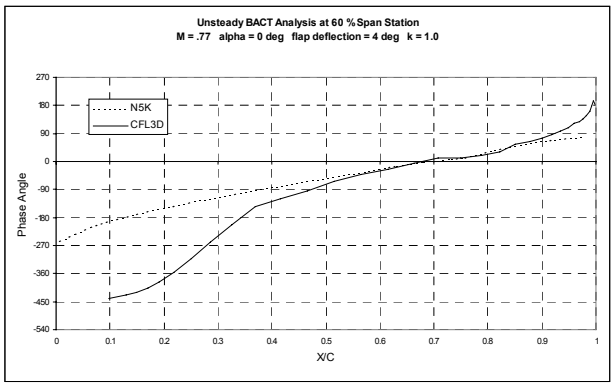

Figure 12- Unsteady Pressure Coefficient for reduced frequency from 0.2 to 1.0

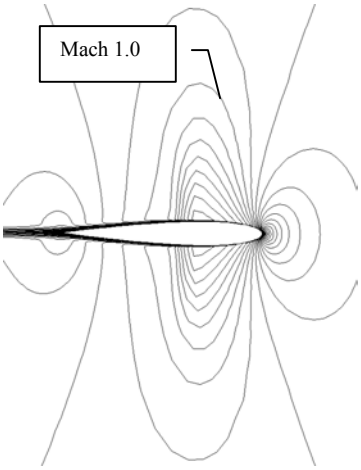

Figure 13- Mach contours for $M_\infty = .82$

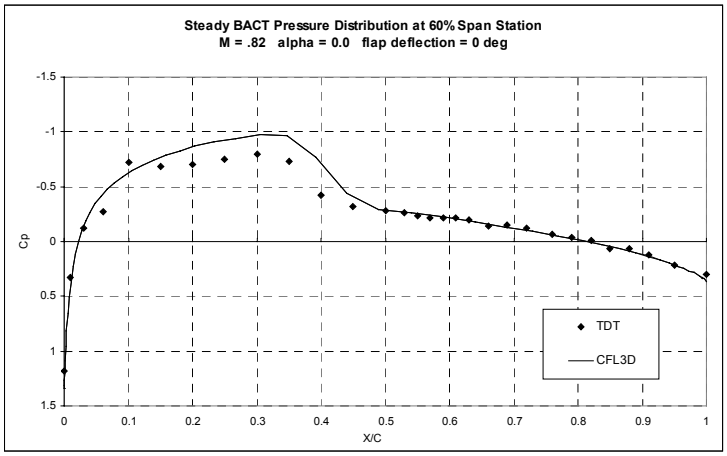

Figure 14- Steady Pressure Coefficient for $M_\infty = .82$

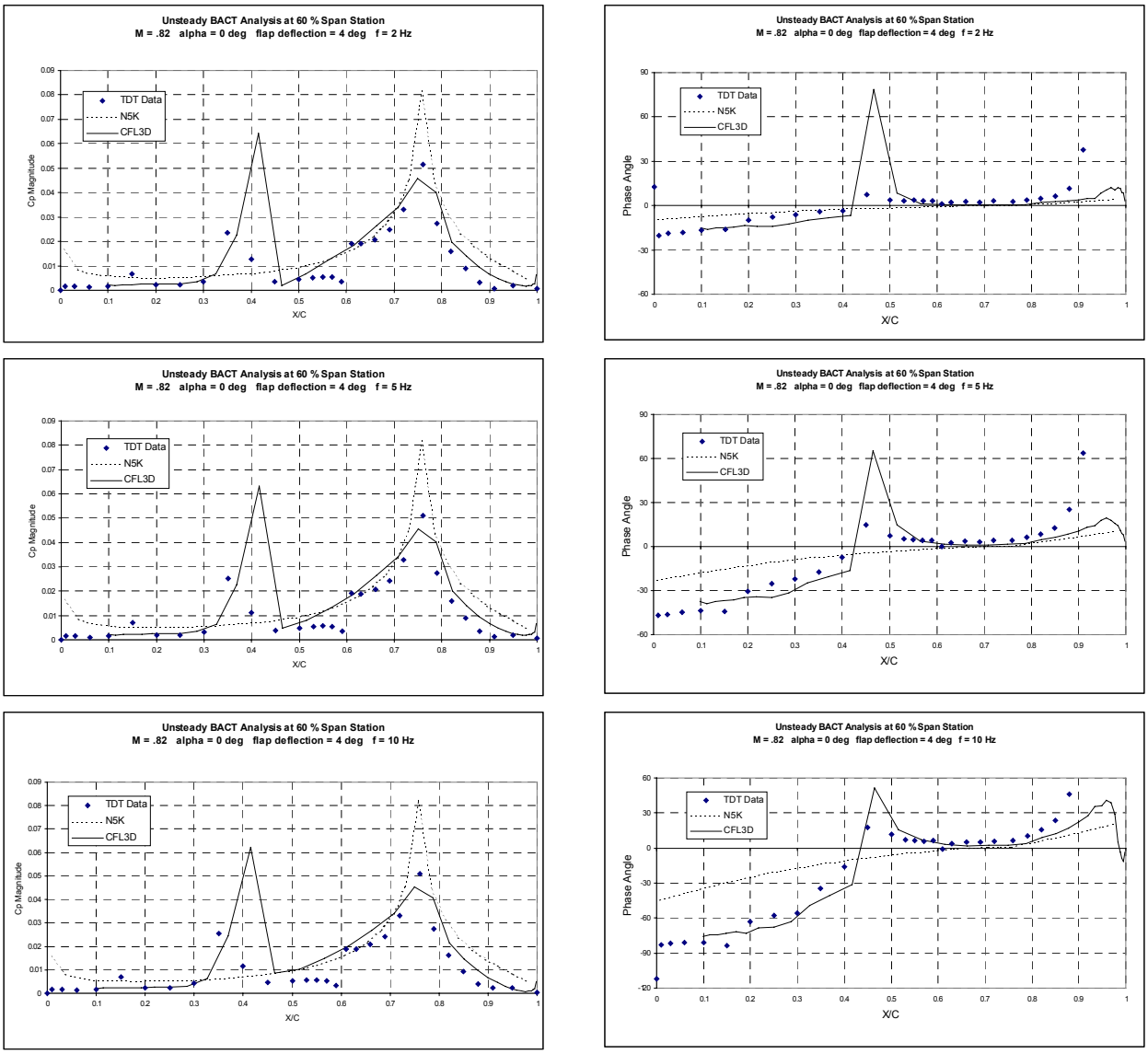

Figure 15- Unsteady Pressure Coefficient from 2 to 10 Hz

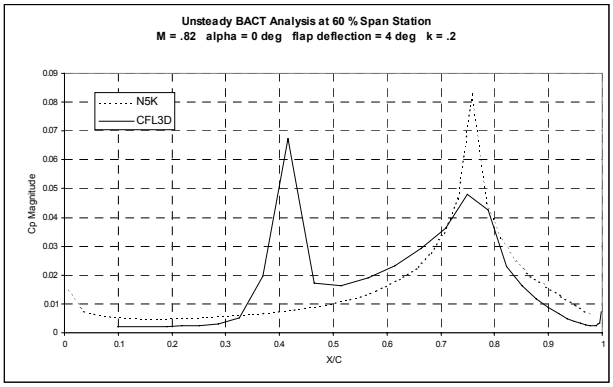

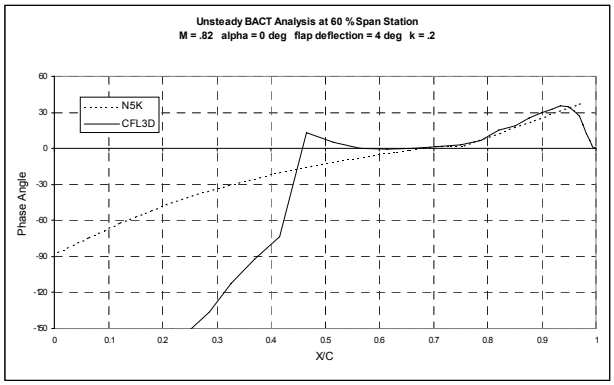

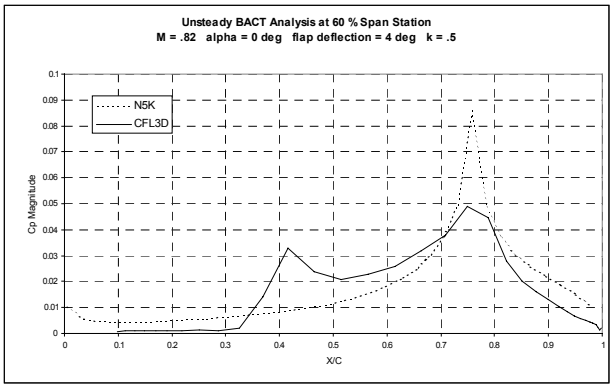

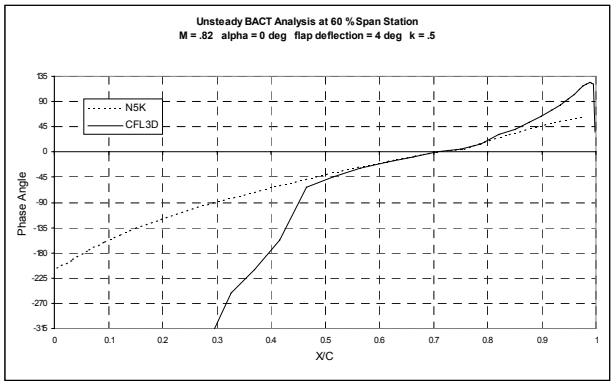

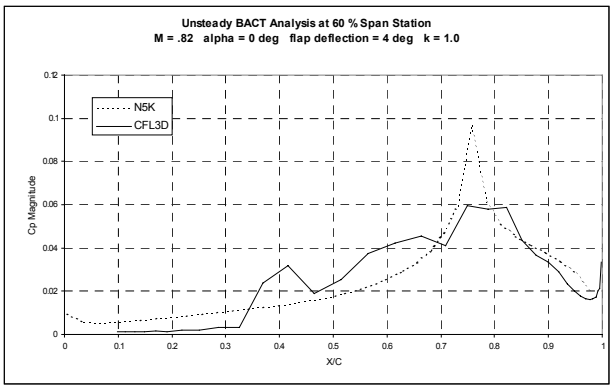

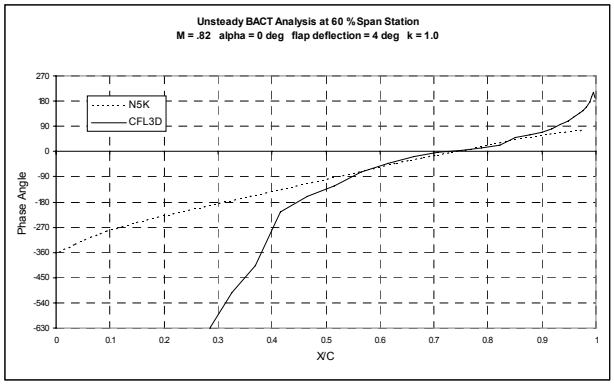

Figure 16- Unsteady Pressure Coefficient for reduced frequency from 0.2 to 1.0

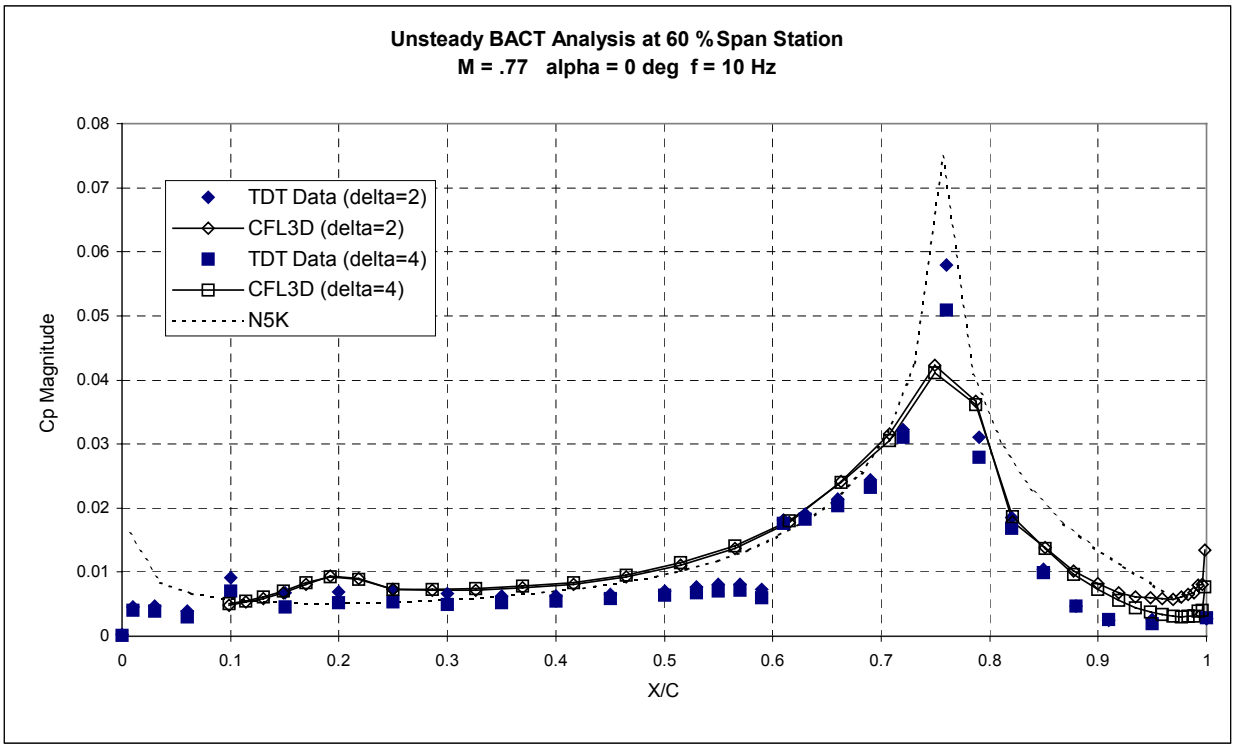

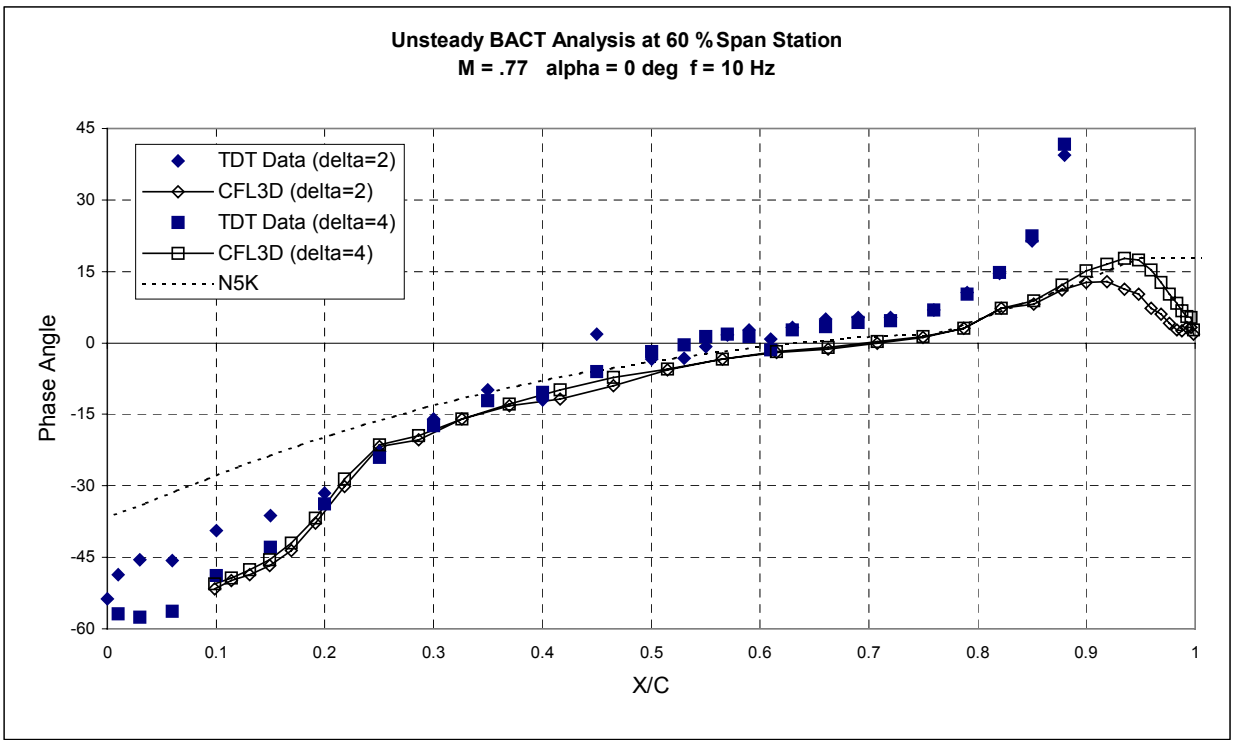

Figure 17- Unsteady Pressure coefficient for flap deflection of 2^{o} and 4^{o} for M_{∞} = .77, f = 10 Hz.

Conclusions

Unsteady aerodynamic analysis has been performed using N5K and CFL3D.AE-BA for cases with varied Mach number and frequency. The results of the study demonstrate excellent correlation of CFD with test data. Inaccuracies in the doublet-lattice results are clearly seen in regions where linear potential theory is not valid.

Correlation to CFD and test data demonstrates the limits of accuracy for the doublet-lattice method. The magnitude results obtained from the doublet-lattice method are acceptable except on the control surface and toward the leading edge. This is in agreement with theory, as viscous effects are relevant on the control surface and thickness effects are relevant toward the leading edge, neither of which are accounted for in linear potential flow. The magnitude results on the flap obtained from the doublet-lattice method are consistently too high when compared to CFD and test data. This will cause doublet-lattice results for both hinge moment and lift to be too large. The doublet-lattice results for magnitude are also consistently too large near the leading edge. This will contribute to linear theory prediction of lift being too large. The doublet-lattice results for phase angle agree well with both CFD and test data except for in supersonic regions and cases with high reduced frequency. The doublet-lattice results predict too small a phase lag in supersonic regions as expected due to the fact that linear potential theory is not valid in regions where compressibility has a significant influence.

Using the results of our study, we are able to see that CFD is significantly better than the doublet-lattice method for predicting control surface aerodynamics. The results from the CFD analysis are clearly in better agreement with the test data than are the results from linear potential theory. Due to better agreement with test data for the pressure magnitude on the flap, we can conclude that CFD analysis will consistently give more accurate hinge moment results. The phase shift due to local supersonic regions is captured excellently by the CFD analysis. The CFD results provide an excellent description of this flow behavior which cannot be accounted for by linear potential theory corrected by steady test data.

Acknowledgements

A version of the CFL3D grid was obtained from the author of reference 4. The grid had been used for ENS3D. Changes were made to include gaps between the flap and the wing and to recluster the grid points. In order to accurately predict viscous effects, more grid points were needed in the normal direction near the surface of the wing. It was also observed that for accurate analysis of deflected flaps, more grid points were needed near the trailing edge of the model in the chordwise direction.

References

1. Rodden, W. P., Taylor P.F., and McIntosh, S. C., Jr., "Further Refinements of the Nonplanar Aspects of the Subsonic Doublet-Lattice Lifting Surface Method," Paper ICAS-96-2.8.2, presented at the 20th Congress of the International Council of the Aeronautical Sciences, Sorrento, Italy, 8-13 September 1996.

2. Rumsey, C., Sanetrik, M., Biedron, R., Melson, N., and Parlette, E., "Efficiency and Accuracy of Time-Accurate Turbulent Navier-Stokes Computations," Computers and Fluids, Vol. 25, No. 2, pp. 217-236, 1996.

3. Schuster, D. M., Beran, P. S., and Huttsell, L. J., "Application of the ENS3DAE Euler/Navier-Stokes Aeroelastic Method," AGARD Report 822, presented at the 85th Meeting of the AGARD Structures and Materials Panel, Aalborg, Denmark, 14-15 October 1997.

4. Scott, R. C., Hoadley, S. T., and Wiseman C. D., "The Benchmark Active Controls Technology Model Aerodynamic Data," AIAA 97-0829, 35th Aerospace Sciences Meeting and Exhibit, January 1997.

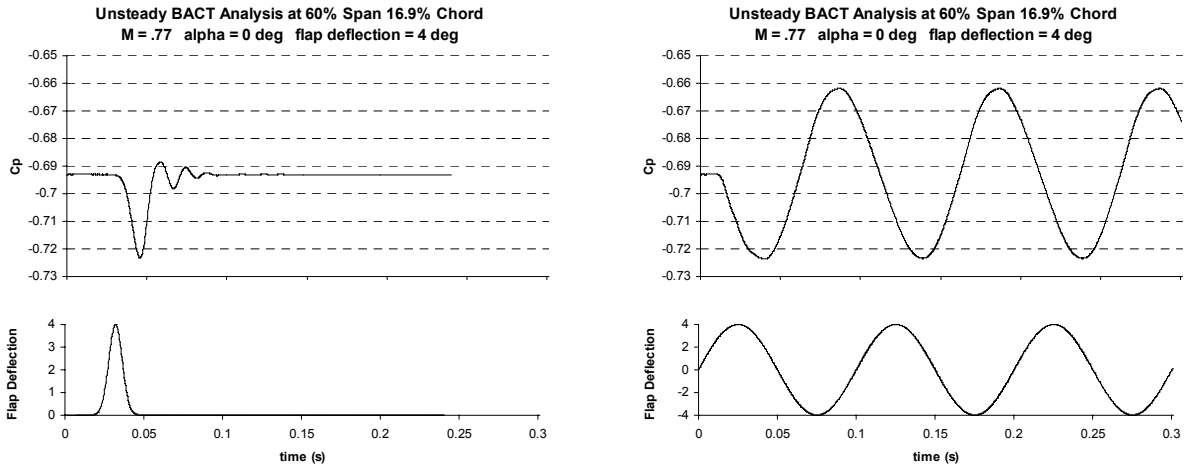

Figure 3- Time History results from CFL3D

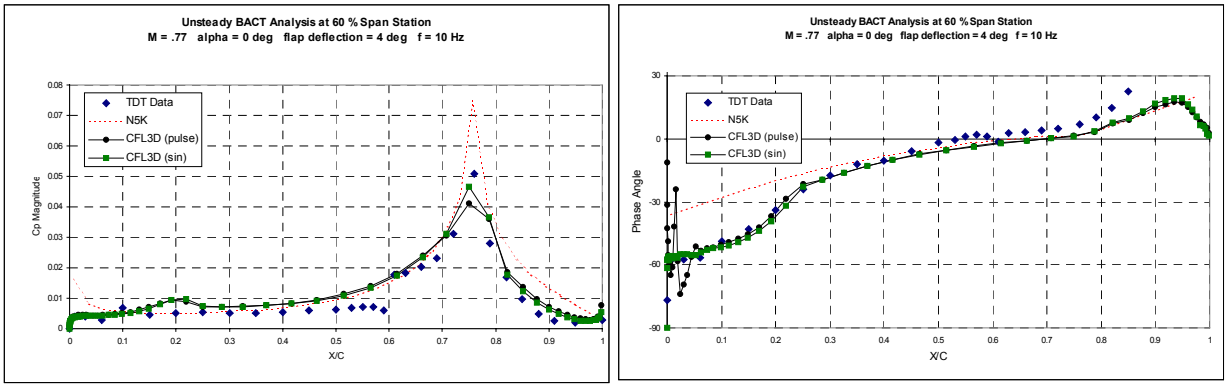

Figure 4- Unsteady Pressure Coefficient Comparison between pulse and sinusoidal input

Figure 2- CFL3D 153x81x45 grid

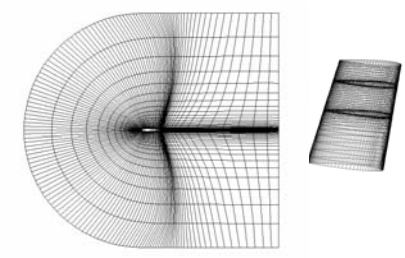

Table 1

	M = 0.65			M = 0.77			M = 0.82			M = 0.90		
	Test	DLM	CFL3D	Test	DLM	CFL3D	Test	DLM	CFL3D	Test	DLM	CFL3D
f = 2 Hz	k = .0248			k = .0209			k = .0197			k = .0179		
	$\delta = 4^o$	X	$\delta = 4^o$	$\delta = 2^o$ $\delta = 4^o$	X	$\delta = 2^o$ $\delta = 4^o$	$\delta = 4^o$	X	$\delta = 4^o$	$\delta = 2^o$	X	$\delta = 2^o$
f = 5 Hz	k = .0620			k = .0523			k = .0492			k = .0448		
	$\delta = 4^o$	X	$\delta = 4^o$	$\delta = 2^o$ $\delta = 4^o$	X	$\delta = 2^o$ $\delta = 4^o$	$\delta = 4^o$	X	$\delta = 4^o$	$\delta = 2^o$	X	$\delta = 2^o$
f = 10 Hz	k = .1240			k = .1047			k = .0983			k = .0896		
	$\delta = 4^o$	X	$\delta = 4^o$	$\delta = 2^o$ $\delta = 4^o$	X	$\delta = 2^o$ $\delta = 4^o$	$\delta = 4^o$	X	$\delta = 4^o$	$\delta = 2^o$	X	$\delta = 2^o$
k = 0.2	f = 16.13 Hz			f = 19.11 Hz			f = 20.35 Hz			f = 22.33 Hz		
		X	$\delta = 4^o$		X	$\delta = 2^o$ $\delta = 4^o$		X	$\delta = 4^o$		X	$\delta = 2^o$
k = 0.5	f = 40.32 Hz			f = 47.76 Hz			f = 50.87 Hz			f = 55.83 Hz		
		X	$\delta = 4^o$		X	$\delta = 2^o$ $\delta = 4^o$		X	$\delta = 4^o$		X	$\delta = 2^o$
k = 1.0	f = 80.64 Hz			f = 95.53 Hz			f = 101.73 Hz			f = 111.66 Hz		
		X	$\delta = 4^o$		X	$\delta = 2^o$ $\delta = 4^o$		X	$\delta = 4^o$		X	$\delta = 2^o$

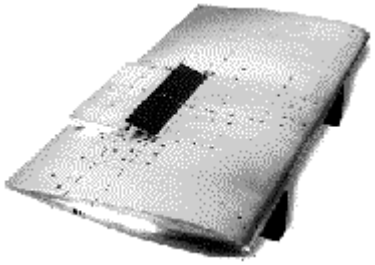

Figure 1- BACT wind tunnel model

Add when visc5 results are in

This is shown conclusively by a case run using both the original grid and a grid with finer chordwise resolution near the hingeline (fig. xxxx).